

Sytske Kamminga Kimball*
University of South Alabama, Mobile, Alabama

1. INTRODUCTION

When a hurricane makes landfall, most damage occurs between the time the 17 ms^{-1} isotach touches the coastline and the time the hurricane center crosses the coast. During this time the hurricane moves from shallow coastal waters to solid land, causing an increase in surface roughness and decrease in surface latent heat fluxes which form the hurricane's energy source over water. These rapidly changing conditions affect the inner-core windfield, and hence the pattern, extent, and intensity of damaging winds and rainfall. The underlying physical processes are complex, occur over a very short time (less than a day), and depend on a myriad of complicating factors such as topography, shape of the coastline, angle of incidence of the storm, speed of motion of the storm, and many more. In order to isolate the effects from just the reduction in surface evaporation and the increase in surface roughness, an idealized modeling study is conducted using a west-east oriented, straight coastline with a land surface of 0.1 m elevation, covered by a constant land-use category in both space and time. Simulations making use of different land-use categories, with different roughness length and moisture content properties, are compared.

2. MODEL CONFIGURATION

The Penn State/NCAR mesoscale model (MM5) is initialized with a southerly geostrophic wind of 8 m s^{-1} . Embedded in this flow is a hurricane vortex with initial minimum surface pressure (PSMIN) of 970.6 mb and 42 km radius of maximum winds (RMW). The intensity and size properties of this vortex are based on the averaged properties of hurricanes making landfall in the north-central Gulf of Mexico during 1988 - 2002. Construction of such a vortex follows the technique outlined in Kimball and Evans (2002). A 42-hour simulation is conducted using a coarse mesh of 9 km horizontal resolution, a nested grid of 3 km horizontal resolution, and 38 vertical levels. The sea surface temperatures (SSTs) in the model are kept constant at 28°C . Convection is parameterized on the coarse mesh using the Kain-Fritsch scheme and is explicit on the fine mesh. Other parameterizations on both meshes include the Goddard Micro-physics (including graupel) scheme, the MRF boundary layer scheme, a 5-layer soil model, and a cloud-radiation scheme.

* Corresponding author address: Sytske K. Kimball
Univ. of S. Alabama, Dept. Of Earth Sciences, Mobile,
Al, 36688 email:skimball@usouthal.edu

3. EXPERIMENTS

A control simulation (noland) consisting of a water surface only is compared to simulations with land use categories of 1) evergreen needleforest (needle) 2) dry land crop pasture (dryland). The physical properties of these categories are listed in Table 1.

Experiment Name	Moisture Availability (%)	Roughness Length (cm)
noland	100	0.06
needle	30	50
dryland	30	15

4. RESULTS

The storm is initially located 400 km south of the straight coastline and moves at around 7 m s^{-1} in a northeasterly direction as a result of the environmental steering flow in combination with the Coriolis force. At $t=22\text{h}$ into the simulation, the storm center crosses the coastline about 400 km east of its original location.

Figure 1 shows the evolution of storm intensity, measured in terms of PSMIN, from $t=6$ to 36h into the simulation. The noland simulation weakens slowly until $t=24\text{h}$ when slow intensification occurs. This storm remains a category 2 hurricane throughout the entire simulation. As expected, the other two storms continue to weaken after their centers cross the coastline at $t=22\text{h}$. The simulation with the larger roughness length (needle) weakens more, again this is expected.

Examination of reflectivity and rainfall distribution and amount (not shown) reveals few differences between needle and dryland. After landfall, the reflectivity in both cases decreases as compared to the noland case. The eye fills in, but a banding structure remains visible throughout the simulation. Maximum hourly rainfall rates in both land cases decrease from around 4cm/h to 1cm/h after the storm centers cross the coastline. In the noland case, the rainfall rates remain at around 4cm/h throughout the simulation. The storms maintain their symmetric reflectivity and rainfall patterns upto 10 hours after making landfall. By $t=33\text{h}$, maximum rainfall rates become concentrated in the southern half (over land) of the storm.

Figure 2 shows the 10 m wind speed and direction for each case at $t=24\text{h}$, i.e. 2 hours after the center has crossed the coastline. In noland, maximum winds of 36

ms^{-1} can be seen in the southeastern quadrant of the storm, while winds of around 30 ms^{-1} are observed in the northwestern quadrant. This asymmetry is a result of the northeast-ward motion of the storm. In both the needle and dryland cases, the strongest winds occur over water where the roughness length is considerable smaller than over land. The larger roughness length in the needle case causes winds over land to be significantly reduced compared to the dryland case. The bold white line (17 ms^{-1} contour) clearly accentuates this. This 6 ms^{-1} difference in windspeed does not significantly affect the surface latent and sensible heat fluxes, which remain similar in magnitude in both land cases (not shown). The only factor that could alter the magnitude of the latent heat flux is the magnitude of the low level wind since the moisture availability is the same in both land cases (Table 1). Hence, the lower intensity of needle compared to dryland (Figure 1) is caused by the effects of increased surface friction.

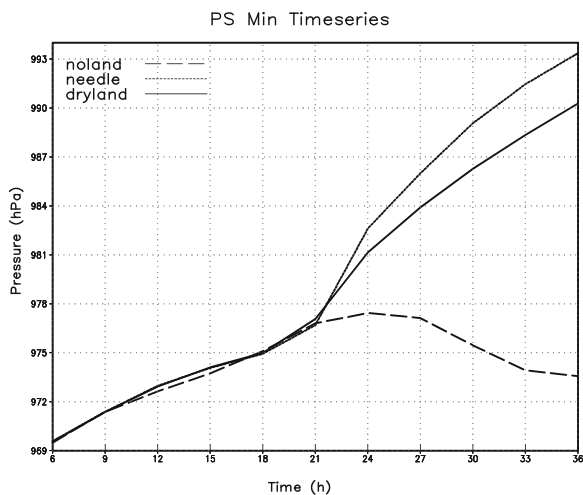


Figure 1: Timeseries of PSMIN for noland, needle, and dryland.

As in the reflectivity and rainfall distribution, the windspeed distribution remains symmetric even after the eyewall is located entirely over land. At $t=30\text{h}$ windspeeds become slightly stronger in the southern half of the storm. By $t=39\text{h}$, windspeeds in the southern half are 4 ms^{-1} stronger than in the northern half of the storm. These asymmetries are minimal compared to real landfalling storms in the north-central Gulf coast, Hurricane Danny (1997) being an extreme example of asymmetry (Blackwell, 2000) observed during landfalling hurricanes. In these simple, idealized simulations variations in topography, landuse, and coastline shape have been removed. This leads to a significant reduction in storm intensity, but a lack of development of significant asymmetry in storm structure.

At the conference additional simulations with different landuse categories will be included.

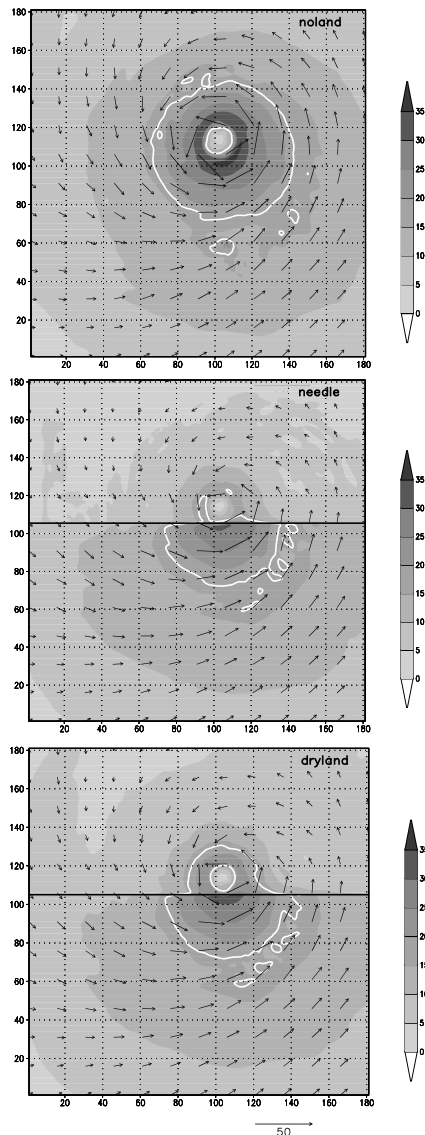


Figure 2: 10 m windspeed (shaded). The white line is the 17 ms^{-1} contour, the black line is the coastline.

Acknowledgements

This work is supported by NSF Award No. ATM-0239492

5. REFERENCES

Blackwell, K. G., 2000: The Evolution of Hurricane Danny (1997) at Landfall: Doppler-Observed Eyewall Replacement, Vortex Contraction/Intensification, and Low-Level Wind Maxima. *Mon. Wea. Rev.*, **128**, 4002–4016.

Kimball S.K. and J. L. Evans, 2002: Idealized numerical modeling of hurricane-trough interaction. *Mon. Wea. Rev.*, **130**, 2210-2227.